Results from a low frequency passive seismic experiment over an oilfield in Abu Dhabi

Mohammed Y. Ali,[1*] Karl A. Berteussen,[1] James Small,[1] Braham Barkat[1] and Okky Pahlevi[1] **present a low frequency passive seismic investigation over an onshore carbonate oilfield in Abu Dhabi to determine the spectral content, apparent velocities, and azimuths of the wavefronts in the *microseism* and *microtremor* bands.**

The ambient noise of the Earth, or background noise, has been studied by numerous researchers over the years (e.g., Kedar and Webb, 2005). At low frequency, the natural activity of the ocean dominates through the *microseisms* band, usually between 5 x 10^{-2} and 10^{-1} Hz for the primary band (Oliver and Ewing, 1957) and 10^{-1} – 2 x 10^{-1} Hz for the secondary band. This produces a noise amplitude peak at ~0.2 Hz, which is visible anywhere on Earth (e.g., Longuet-Higgins, 1950). At high frequencies (> 1 Hz), the seismic noise field is mainly dominated by cultural or wind-generated noise (e.g., Peterson, 1993), with wind noise being the predominant high-frequency source at remote sites (e.g. Withers et al., 1996) and traffic and factories being the major source of noise in urban sites (Marzorati and Bindi, 2006).

For several years a narrow band of *microtremor* (~2 – 5 Hz) signals with a peak ~ 3 Hz has been observed over a number of hydrocarbon reservoirs, including some oilfields in Abu Dhabi (Dangel et al., 2003; Holzner et al., 2005; Akrawi and Bloch, 2006; Walker, 2008; Hanssen and Bussat, 2008). These observations have been interpreted to suggest that the low frequency signals recorded diminish towards the rim of an oil reservoir and are totally absent above non-reservoir locations. Furthermore, it has been suggested (e.g., Holzner et al., 2005; Saenger, et al. 2007; Graf et al. 2007) that the detection of these low frequency wavefield can be a useful tool in such diverse applications as the reconnaissance of frontier exploration areas, optimization of borehole placement, reservoir monitoring, and as a complementary tool for structural imaging to reduce

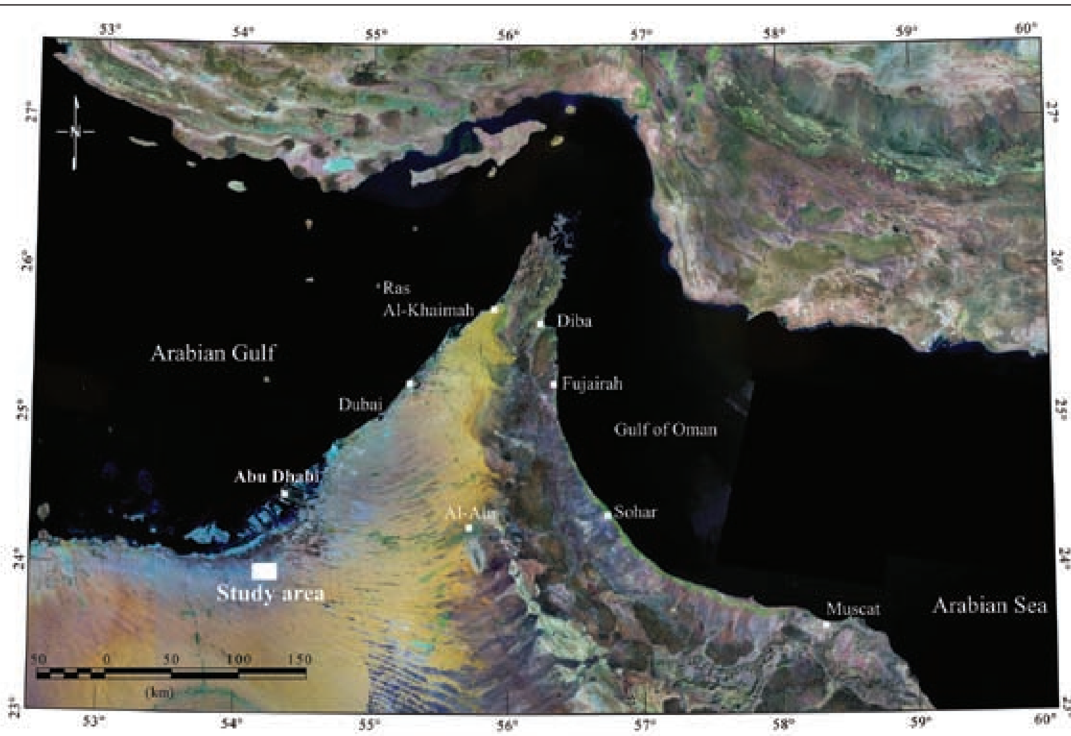

***Figure 1a** Regional satellite map showing the study area.*

[1] *The Petroleum Institute, P.O. Box 2533, Abu Dhabi, UAE.*
**Corresponding author, E-mail: mali@pi.ac.ae*

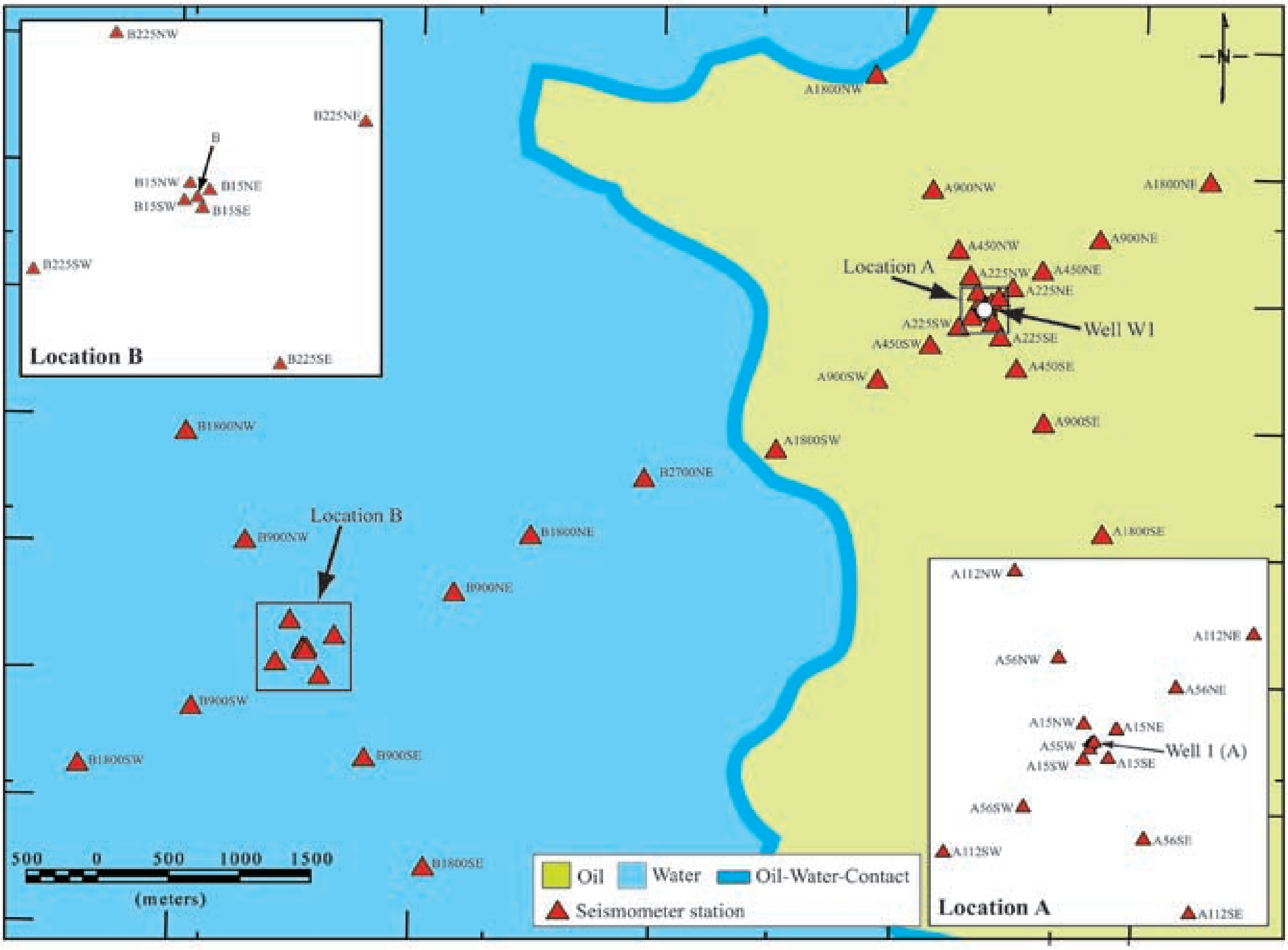

Figure 1b *Location map of the experiment showing positions of seismometers and oil-water contact of the oilfield.*

drilling risk and assist with well positioning. Some studies (e.g., Dangel et al., 2003; Holzner et al., 2005; Akrawi and Bloch, 2007; Walker, 2008) have even suggested a linear relationship between the observed signal and the total thickness of hydrocarbon-bearing layers.

While the actual causes of this low frequency wave phenomena are still not well understood, it has been suggested (e.g., Holzner et al., 2005; Saenger, 2007; Graf et al., 2007; Walker, 2008; Holzner, et al., 2009) that these signals are the result of resonance amplification or resonance scattering by the hydrocarbons present in subsurface reservoirs. These models assume that non-linear behaviour of the interaction between liquid hydrocarbons, water, and the pore-rock materials in the reservoirs can distort the normal signature of the Earth's natural ambient vibration spectra. Recently, Steiner et al. (2008) has applied time reverse modelling to suggest that the hydrocarbon reservoir zone itself is the origin of the low-frequency spectral anomalies.

Berteussen et al. (2008) have shown that the observed low frequency signals appear to be surface waves. In another study, Hanssen and Bussat (2008) analyzed the low frequency ambient noise detected over an oilfield in the Sahara desert of Libya and suggested that noise from human activities could produce a similar signal as the low frequency signal presumed to be generated by the hydrocarbon reservoir.

In this paper we present the results of a low frequency passive seismic investigation which was carried out over an onshore carbonate oilfield in Abu Dhabi to determine the spectral content, apparent velocities, and azimuths of the wavefronts in the *microseism* and *microtremor* bands. This study is a follow up of the work presented by Ali et al. (2007).

Study area and data acquisition

The experiment was carried out between 21 May and 17 June of 2007 over an onshore oilfield located ~50 km southwest of Abu Dhabi city (Figure 1a). The oilfield was selected as a suitable site for the experiment because it has a clear and well-defined oil-water contact (OWC) mapped from 3D seismic and well data.

During the acquisition of the data a powerful tropical cyclone (Cyclone Gonu) struck the coast of Oman. Cyclone Gonu developed in the eastern Arabian Sea on 1 June 2007

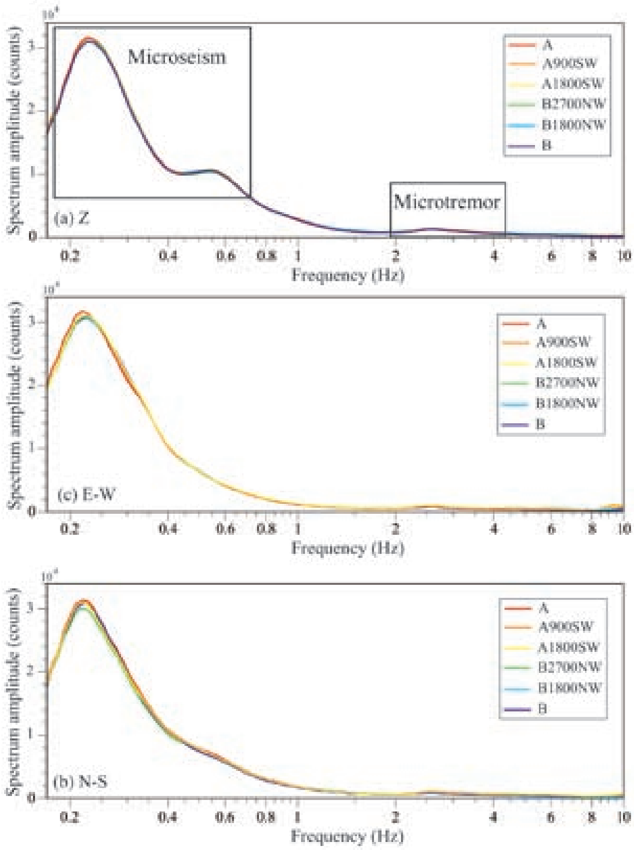

Figure 2 *Ambient wavefield noise recorded from Location A to B on 7 June 2007 showing typical spectral amplitudes of microseism and microtremor signals. (a) Vertical component (b) East-west component (c) North-south component. Microseism and microtremor signals were observed on all three components (vertical, north-south, and east-west) of the seismometers at all recording stations.*

to attain peak winds of 240 km/h on 3 June, then struck the eastern coast of Oman on 5 June with winds of 150 km/h to become the strongest tropical cyclone to hit the Arabian Peninsula in recorded times (De Bhowmick et al., 2007). It then turned northward into the Gulf of Oman, and dispersed after moving ashore along the southern Iranian coast on 7 June 2007.

The experiment included the acquisition of 11 arrays of varying aperture sizes (15–1800 m) with typically 24 hours recording time each. The arrays were centred at locations A and B (Figure 1b). Location A is situated over the maximum oil column (>120 ft) of the reservoir, whereas location B was positioned over an area that presumably contained no oil. In addition, a 2D profile running from location A to location B was acquired.

The wavefield signals were recorded using six ultra sensitive 3-component seismometers (Guralp CMG-6TD). The seismometers were placed on concrete slabs in pits of ~50 cm deep and oriented to the geographic north. The sensors were then covered and buried for firm ground contact and wind shielding.

Various signal analysis techniques were applied to the data including time series, power spectral density, and time frequency analyzes. A processing window of 60 seconds and 5% cosine taper were applied to the data to reduce spectral leakage. Fourier amplitude spectra were analyzed both without smoothing and with the smoothing procedure described by Konno and Ohmachi (1998) using a b-value of 40. The mean of the signal was removed and excessively noisy sections were excluded from the analyses prior to stacking the data.

Ambient earth noise sources

The ambient noise levels observed at the site generally fall into two frequency bands: *microseism* (~0.16-0.6 Hz) and *microtremor* (2.5-3 Hz). In this section we detail the noise spectra amplitudes estimated for the site within these bands.

Microseism

Figure 2 illustrates that the noise spectrum is dominated by a strong and easily recognizable *microseism* peak called the double-frequency peak (Longuet-Higgins, 1950) at ~0.25 Hz with a secondary peak at ~0.55 Hz. These *microseism* events are believed to occur as a result of the interaction between two same frequency ocean swells that are propagating in opposite directions (Longguet-Higgins, 1950; Kedar and Webb, 2005). *Microseism* energy propagates primarily as fundamental Rayleigh waves which do not attenuate rapidly (Bromirski and Duennebier, 2002). As a result, the double-frequency *microseism* is observed in the background noise at all sites worldwide including those at continental sites far removed from the coast (Peterson, 1993). The level of the double-frequency *microseism* depends on several factors including the amplitude of the interacting ocean waves, the size of the area of interaction, and the propagation characteristics of the wavefield (Longuet-Hinggins, 1950; Bromirki and Duenebier, 2002).

The correlation between the double-frequency *microseism* peak and the presence of ocean storms is supported by the temporal variation of spectral levels of the double-frequency *microseism* observed during the approach of Cyclone Gonu. Figure 3a illustrates that the spectral amplitudes of ambient noise level between 0.16 and 0.25 Hz increased when Cyclone Gonu approached the coast of Oman (4-7 June). The spectral amplitudes reached a maximum on 6 June, then dropped off as the cyclone passed the region. The increased spectral amplitudes recorded are consistent with increased intensity and proximity of the cyclone as shown on the satellite image in Figure 4. In addition, we observe that, as the cyclone develops, the spectral levels are initially highest at frequencies in the range of ~0.25 Hz. However, as the storm intensifies, the wave energy peak has shifted towards the lower frequencies ~0.18 Hz. This is in agreement with other studies (e.g. Marzorati and Bindi, 2006) which have observed similar phenomena.

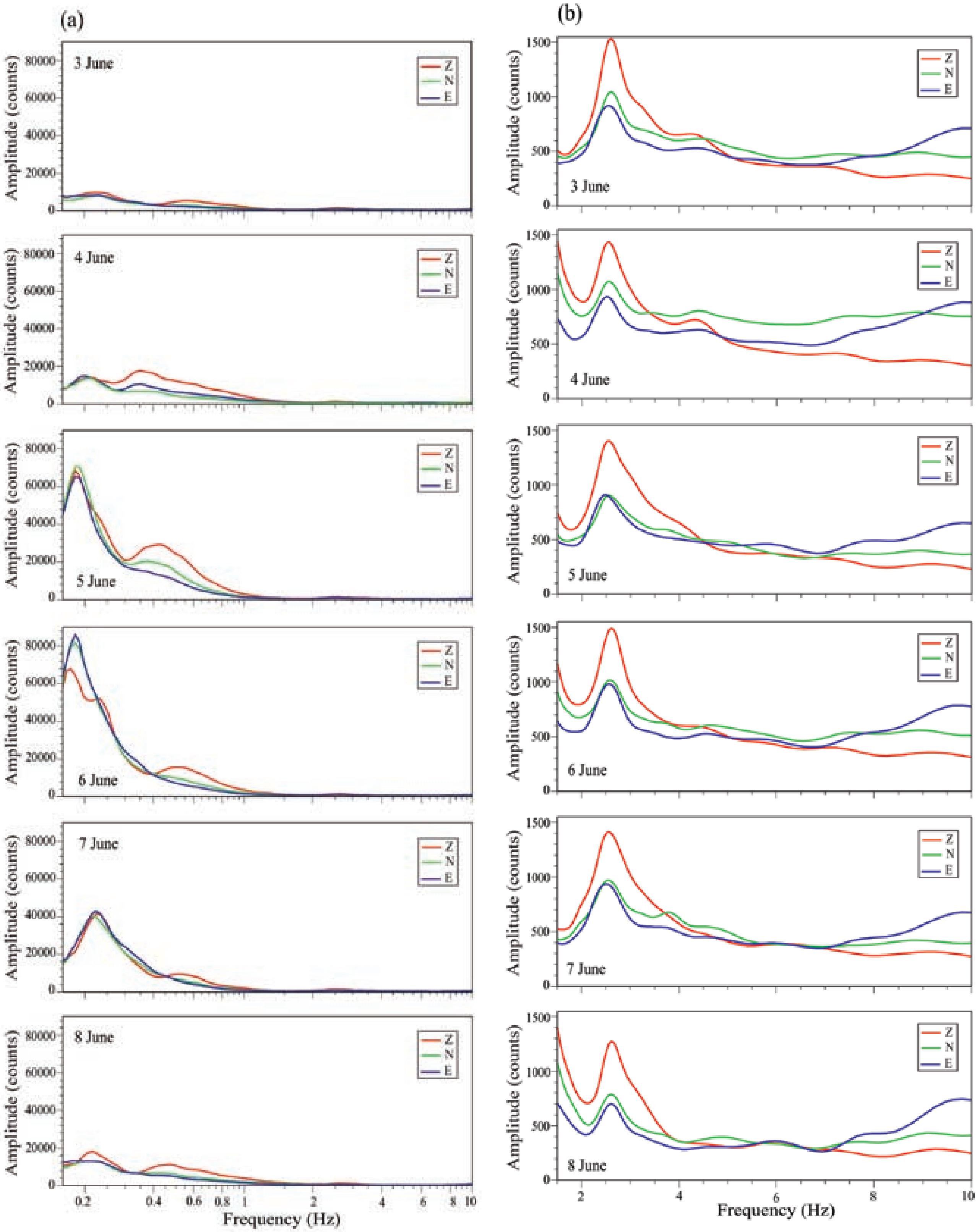

Figure 3 Comparison of spectral amplitudes at location A during midday of the time interval of Cyclone Gonu. (a) Logarithmic frequency scale from 0.1 –10 Hz to illustrate the microseism event. (a) Linear frequency scale from 1.5–10 Hz to show the microtremor event. The spectral amplitudes of microseisms increased dramatically when Cyclone Gonu approached the coast of Oman, whereas the microtremor signal remained unchanged.

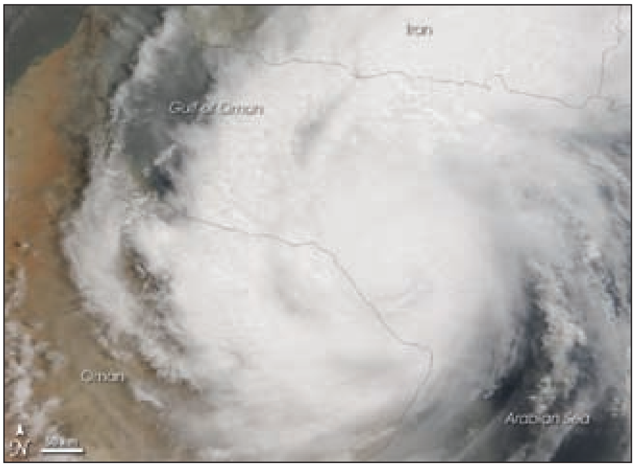

Figure 4 *Satellite image of Oman and surrounding areas on 6 June 2007 showing Cyclone Gonu striking the eastern coast of Omani. (Source: http://earthobservatory.nasa.gov/NaturalHazards/view.php?id=18442).*

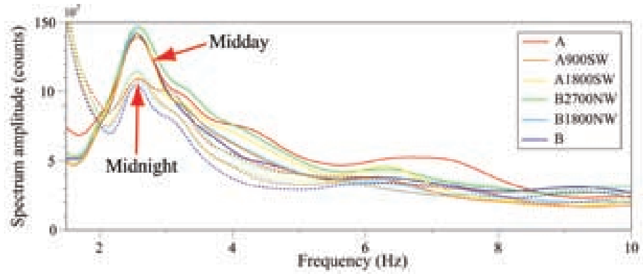

Figure 5 *Spectral amplitudes of the vertical sensors located along a profile from location A to B on 7 June 2007 (For location see Figure 1b) showing microtremor signal (~2.7 Hz) over all stations including those on the oil reservoir (location A) and those on the water saturated zone (location B). Microtremor signal during midday is much stronger compare to the midnight microtremor signal.*

Microtremor

Figure 5 shows the spectral amplitude of the 2D profile running from location A to location B. The figure shows a distinct spectral anomaly, referred to as *microtremor* in the frequency band of ~2-3 Hz. The *microtremor* signal is observed over all recording stations including those on the oil reservoir (location A) and those over the water saturated zone (location B). In addition, all three components (vertical, north-south, and east-west) of the seismometers recorded the signal (Figure 2).

Figure 3b also indicates that there is no clear relationship between the strength of the *microtremor* and the *microseism* signals. During the period in which Cyclone Gonu was battering the Omani coast the *microseism* signal increased by a factor of ~10, whereas the *microtremor* signal remained seemingly unchanged. Hanssen and Bussat (2008) have also noted that there is no correlation between the low frequency (1-6 Hz) band and *microseism* signal (< 0.25 Hz). This finding contradicts Holzner et al. (2005) and Holzner et al. (2009) who have suggested that the driving force of the low frequency signals is the *microseism* events.

Moreover, the *microtremor* signal appears to exhibit strong diurnal variations. During day time periods a strong *microtremor* signal appears on all three components of all sensors (vertical, north-south, and east-west), whereas during the night only weak signals were detected (Figures 5 and 6). These observations suggest that the source responsible for the *microtremor* signal is possibly correlated with meteorological or anthropogenic noises, or perhaps with solar heating of

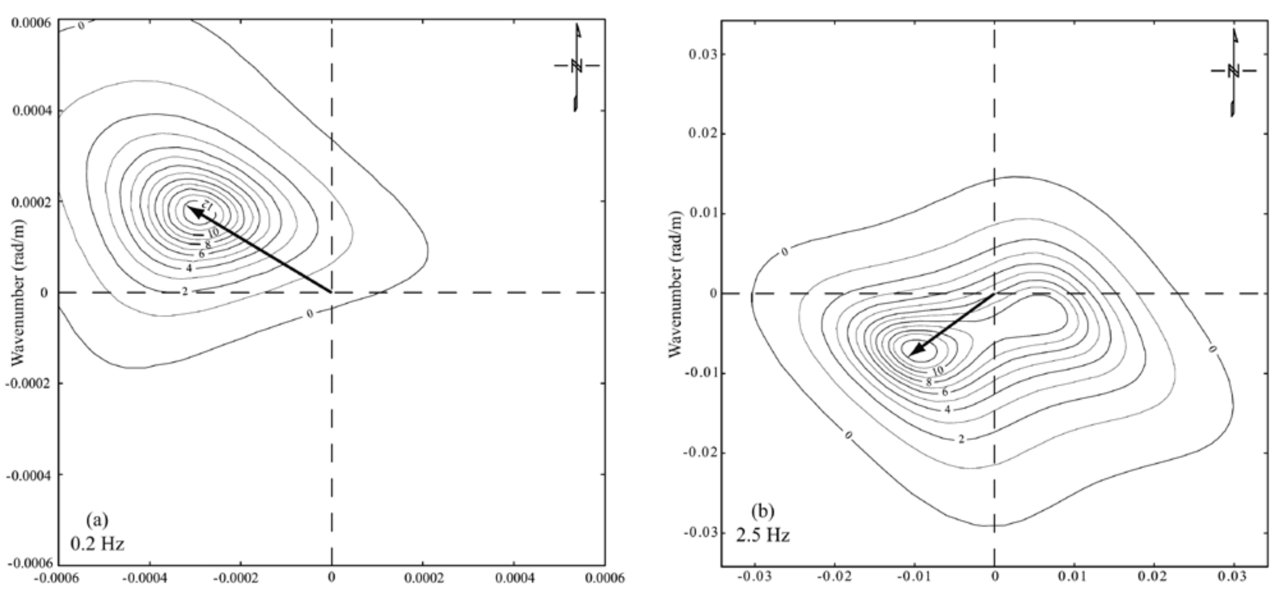

Figure 6 *Time frequency display for data recorded from the vertical component of the seismometer at location A on 26 May 2007. The microtremor signal exhibit strong diurnal variations with a strong signal during the day and a weaker signal at night. At high frequencies (> 6 Hz) the ambient noise is contaminated with high amplitude wind or cultural noise.*

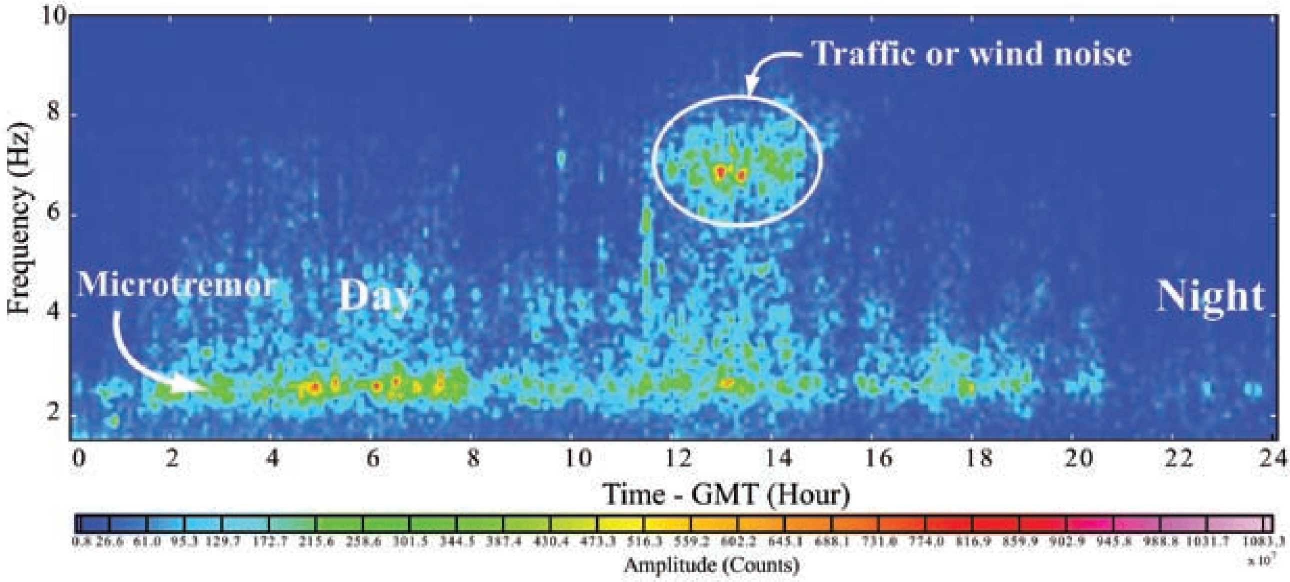

Figure 7 Energy response in slowness space for arrays of varying aperture sizes at location A. (a) Centre frequency = 0.2 Hz, array radius = 1800 m. The propagation azimuth (from the source) of the wavefront is ~300° (from north) with apparent velocity of ~3600 m/s (apparent velocity = 2ϖf/|k|, and wavelength, λ= 2ϖ/|k|, where f = frequency and k= wavenumber). (b) Centre frequency = 2.5 Hz with array radius of 56 m. The propagation azimuth of the wavefront is 230° with apparent velocity of 1300 m/s. For locations of the sensors see Figure 1b.

the desert. Furthermore, the fact that all three sensor components recorded the *microtremor* signal confirms that the signal cannot be a P-wave travelling directly up from below the sensors (i.e., from the hydrocarbon reservoir). Therefore, the *microtremor* signal is interpreted as being surface waves, or a combination of shear and surface waves.

However, the coupling of anthropogenic (e.g., traffic, production installations) and local meteorological energy (e.g., wind effects) into the earth may affect the signal particularly at higher frequencies. For example, Figure 6 shows that the ambient noise is contaminated with high amplitude wind or cultural noise in the frequency range of 6-8 Hz. Regional earthquakes can also contaminate the signal by generating low frequency noise. Similar findings have been published from other studies. For example, in a study carried out on an oilfield in Libya, Hanssen and Bussat (2008) correlated the *microtremor* signal with surface waves caused by anthropogenic noises (e.g. production facilities, traffic), resonance frequency of the unconsolidated material in the area, and topography (height of sand dunes).

Array analysis

High-resolution frequency-wave number (*f-k*) spectral analysis (Capon, 1969) is used to determine the apparent velocities and azimuths of the wavefronts. Figure 7 shows the slowness maps for two frequency bands (top: centre frequency = 0.2 Hz bottom: centre frequency = 2.5 Hz) at location A with varying apertures of 1800 m and 56 m respectively. The figure illustrates that the propagation azimuth (from the source) of the 0.2 Hz wavefront is ~300° (front north) with apparent velocity of ~3600 m/s. The wavefront is interpreted as a *microseism* event generated by wave activity in the Indian Ocean/Arabian Sea. The higher apparent velocity indicates that the wavefield has interacted with deeper more compacted carbonate rocks.

The propagation azimuth of the 2.5 Hz wavefront is measured as 230° with apparent velocity of 1300 m/s. The study area is composed of a few metres of unconsolidated sand and sabkha which lay directly over relatively hard carbonate layers having P-wave velocities far above 1300 m/sec. Therefore, the observed wavefront cannot be an ordinary P-wave which has originated from the subsurface hydrocarbon reservoir. If the recorded waves were coming from directly below the array, then they would arrive simultaneously at all seismometers (i.e., the apparent velocity would be infinite and the azimuth undefined). Therefore, on the basis of these observations, the origin of the low frequency ambient noise is interpreted as an S-type wave or more likely some sort of surface-coupled wave that has originated from the waters of the Arabian Gulf. This analysis is consistent with the interpretation drawn from the spectral amplitude analyses, but is in apparent contrast with other studies (e.g. Dangel et al., 2003; Holzner et al., 2005; Walker, 2008) which have attributed the spectral peaks of the *microtremor* events with the location of subsurface hydrocarbon reservoirs.

Conclusions

Observations from the analyses of the spectral amplitudes and high-resolution *f-k* studies of the data have revealed the following results:

- Double-frequency *microseism* signals are observed within the frequency band of 0.16-0.25 Hz. The spectral amplitudes of the *microseism* correlate well with the appearance of Cyclone Gonu that developed in the Indian Ocean/Arabian Sea during the survey. The spectral amplitudes of the *microseism* increase as Cyclone Gonu approached the coast of Oman then drop off once the cyclone has passed the region.
- *Microtremor* signals are observed in the frequency band of ~2-3 Hz. During the day all sensor components (vertical, north-south and east-west) recorded strong *microtremor* signals, whereas during the night the signals were consistently weaker. The *microtremor* signal is interpreted as surface waves which have been modified by meteorological and/or cultural noises.
- There is no apparent correlation between the *microtremor* and *microseism* signals, and therefore, the driving force of the *microtremor* signal cannot be the *microseism* events.
- The apparent velocity and propagation azimuth (from the source) of *microseism* signal are 3600 m/s and 300° respectively for Location A. These results suggest that the source of the *microseism* is the ocean swells of the Indian Ocean/Arabian Sea.
- The apparent velocity and propagation azimuth for the *microtremor* signal recorded at location A are ~1300 m/s and 230° respectively. These results indicate that the observed *microtremor* signals originate from some type of surface waves having an azimuth directed from the nearest coastline in the area (i.e., the Arabian Gulf).

Acknowledgements

We are grateful to the Oil Subcommittee of the Abu Dhabi National Oil Company (ADNOC) and its operating companies (OpCos) for sponsoring this project. We thank Marwan Haggag for his logistical support of the fieldwork and in coordinating the project.

References

Ali, M. Y., Berteussen, K., Small, J. and Barkat, B. [2007] A low frequency, passive seismic experiment over a carbonate reservoir in Abu Dhabi. *First Break*. **25**, 71-73.

Akrawi, K. and Bloch, G. [2006] Application of passive seismic (IPDS) surveys in Arabian Peninsula. *EAGE Workshop on Passive Seismic: Exploration and Monitoring Applications,* Dubai. Extended Abstract, A28.

Berteussen, K., Ali, M. Y., Small, J. and Barkat, B. [2008] A Low Frequency, Passive Seismic Experiment over a Carbonate Reservoir in Abu Dhabi – Wavefront and Particle Motion Study. *70th EAGE Conference & Exhibition*, Rome. Extended Abstract, B046.

Bromirski, P.D. and Duennebier, F.K. [2002] The near-coastal microseism spectrum: spatial and temporal wave climate relationships. *Journal of Geophysical Research*, **107**, 5.1-5.20.

Capon, J. [1969] High-resolution frequency-wavenumber spectrum analysis. *Proc. IEEE*, **57**, 1408-1481.

Dangel, S., Schaepman, M.E., Stoll, E.P., Carniel, R., Barzandji, O., Rode, E.D. and Singer, J.M. [2003] Phenomenology of tremor-like signals observed over hydrocarbon reservoirs. *Journal of Volcanology and Geothermal Research*, **128**, 135-158.

De Bhowmick, A.K., Thani, M.A. and Al-Rawahi, Y. [2007] Cyclone 'GONU' and reliability of main interconnected transmission system of Oman. *AUPEC Conference*, doi: 10.1109/AUPEC.2007.4548022

Graft, R., Schmalholz, S.M., Podladchikov, Y. and Saenger, E.H. [2007] Passive seismic low frequency spectral analysis: Exploring a new field in geophysics. *World Oil*, January, 47-52.

Hanssen, P. and Bussat, S. [2008] Pitfalls in the analysis of low frequency passive seismic data. *First Break*, **26**, 111-119.

Holzner, R., Eschle, P., Zurcher, H., Lambert, M., Graf, R., Dangel, S. and Meier, P.F. [2005] Applying microtremor analysis to identify hydrocarbon reservoirs. *First Break*, **23**, 41-46.

Holzner, R., Eschle, P., Dangel, S., Frehner, M. Narayanan, C. and Lakehal, D. [2009] Hydrocarbon microtremors interprted as nonlinear oscillations driven by oceanic background waves. *Communications in Nonlinear Science and Numerical Simulations*, **14**, 160-173.

Kedar, S. and Webb, F. [2005] The ocean's seismic hum. *Science*, **307**, 682-683.

Konno, K. and Ohmachi, T. [1998] Ground-motion characteristics estimated from spectral ratio between horizontal and vertical components of microtremor. *Bulletin of the Seismological Society of America*, **88**(1), 228-241.

Longuet-Higgins, M. [1950] A theory of the origin of microseisms. *Phil, Trans. Royal Soc. London*, Series A., Mathematical and Physical Sciences, 243, 1-35.

Marzorati, Z. and Bindi, D. [2006] Ambient noise levels in north central Italy. *Geochemistry Geophysics Geosystems*, **7**(9), Doi:10.1029/2006GC001256.

Oliver, J. and Ewing, M. [1957] Microseisms in the 11- to 18-second period range. *Bull. Seismol. Am.,* **47**(2), 111-127.

Peterson, J. [1993] Observations and modeling of seismic background noise. *US Geological Survey*, Open File Report, 93-322.

Saenger, E.H., Schmalholz, S.M., Podladchikov, Y., Holzner, R., Lambert, M., Steiner, B., Quintal, B. and Frehner, M. [2007] Scientific strategy to explain observed spectral anomalies over hydrocarbon reservoirs generated by microtremors. *70th EAGE Conference & Exhibition*, London. Extended Abstract, A033.

Steiner, B., Saenger, E.H. and Schmalholz, S.M. [2008] Time reverse modelling of low-frequency microtremors: Application to hydrocarbon reservoir localization. *Geophysical Research Letters*, **35**, L03307.

Walker, D. [2008] Recent developments in low frequency spectral analysis of passive seismic data. *First Break*, **26**(2), 69-77.

Withers, M. M., Aster, R. C., Young, C. J. and Chael, E. P. [1996] High-frequency analysis of seismic background noise as a function of wind speed and shallow depth. *Bulletin of the Seismological Society of America*, **86**(5), 1507-1515.